American Mineralogist, Volume 73, pages 405–412, 1988

Ingersonite, a new calcium-manganese antimonate related to pyrochlore, from Långban, Sweden

Pete J. Dunn
Department of Mineral Sciences, Smithsonian Institution, Washington, D.C. 20560, U.S.A.
Donald R. Peacor
Department of Geological Sciences, University of Michigan, Ann Arbor, Michigan 48109, U.S.A.
Alan J. Criddle, Chris J. Stanley
Department of Mineralogy, British Museum (Natural History), London SW7 5BD, England

Abstract

Ingersonite, $Ca_3MnSb_4O_{14}$, is hexagonal, space group $P3m$, $P32$, $P\bar{3}m$, $P3_12$, or $P3_22$, with $a = 7.287(3)$, $c = 17.679(9)$ Å, $V = 813.0(6)$ Å^3, $Z = 3$. The strongest X-ray diffractions [d (I/I_0) (hkl)] are 2.971 (100) (222), 1.55 (80) (226), 1.819 (70) (440), 5.92 (60) (111), and 3.10 (50) (113). The chemical composition, determined by microprobe analysis, is FeO 0.2, MgO 0.0, CaO 15.9, Sb_2O_5 74.7, MnO 9.4, sum 100.2 wt%; F is present, and the content varies from 1.4 to 3 wt%. These data, combined with the cell parameters, indicate that ingersonite is isotypic with pyrochlore and romeite. Ingersonite occurs as irregular aggregates of subhedral crystals with calcite, clinohumite?, jacobsite, and an unnamed mineral at the Långban mine, Värmland, Sweden. It is transparent to translucent, has a vitreous luster, and is uniaxial negative. In reflected plane-polarized light, it is light gray, sometimes with a slight yellowish cast imparted by characteristic yellow and white internal reflections. Luminance values [Y (%)], computed from visible spectrum reflectance measurements, are about 10% in air and 2 to 3% in Zeiss oil (N_D 1.515). Indices of refraction calculated from the reflectance spectra are given; $r < v$.

Introduction

In 1985, Roland Eriksson of Långban, Sweden called an unknown yellow mineral to the attention of one of the authors (P.J.D.). The X-ray powder photograph of this mineral resembled that of romeite, but exhibited distinct differences. A detailed examination of this new phase indicated that it is hexagonal, with Mn:Ca near 1:3, and is a new mineral species. We have named this new mineral species *ingersonite* in honor of Dr. H. Earl Ingerson, distinguished geochemist of Swedish ancestry, and presently Professor Emeritus at the University of Texas. The species and the name were approved by the Commission on New Minerals and Mineral Names, IMA. Type material is deposited in the Smithsonian Institution under catalogue number 163012, and at the British Museum (Natural History) under catalogue number BM 1986, 410: E.1177.

Occurrence

Ingersonite was found on the dumps at the Långban mine, Värmland, Sweden, and nothing is known of the specific geologic relations of its occurrence. The sole sample we have studied, 5 × 4 × 2 cm in size, consists of fine-grained calcite with two opaque minerals (jacobsite and filipstadite) as very fine grained crystals irregularly distributed throughout the calcite. The specimen has no preferred orientation. Ingersonite occurs sparsely as irregular yellow aggregates, few in number; hence, it is a rare mineral. More detailed data on the textures are given below. There is much visual similarity between ingersonite and other yellow minerals from Långban, so it is possible that some specimens of ingersonite may have been misidentified. However, intensive searches of systematic museum colllections failed to find additional ingersonite specimens.

Chemical composition

There was insufficient material for a wet-chemical analysis, and ingersonite was chemically analyzed using electron microprobes. A wavelength-dispersive microprobe scan indicated the absence of elements with atomic number greater than 8 other than those given below. The resultant analyses, together with standards used, are presented in Table 1.

The crystal structure of pyrochlore, with which ingersonite is isotypic as discussed below, has two cation sites of equal rank, one having eightfold coordination and the other octahedral coordination. The ideal formula of pyrochlore, as represented by most synthetic phases with the pyrochlore structure (Subramanian et al., 1983) and approached by most natural pyrochlore-family minerals, is $A_2B_2O_7$. The A site is commonly occupied by large cations such as Cd^{2+}, Ca^{2+}, and Mn^{2+}, whereas Sb^{5+} occupies the octahedrally coordinated B site. Because the an-

0003–004X/88/0304–0405$02.00

TABLE 1. Microprobe analyses of ingersonite

	Grain 1*	Grain 2*	Grain 3**
CaO	15.9	16.7	19.9
MnO	9.4	9.4	9.1
MgO	0.0	0.0	0.3
FeO	0.2	0.0	0.3
Sb_2O_5	74.7	73.8	72.6
Total	100.2	99.9	102.2†

* Cambridge Instruments Microscan IX electron microprobe, 20 kV. Standards: Pure Sb, Al, and Mn, CaF, $MgSiO_4$, $MgCrO_4$, and FeS.

** ARL-SEMQ electron microprobe, 15 kV, 0.025-μA sample current. Standards: synthetic Sb_2O_3 (Sb), manganite (Mn), fluorapatite (F), hornblende, (Ca, Mg, Fe). Data corrected with a modified version of the MAGIC-4 program.

† F is present, but inhomogeneous; value is 1.4 to 3 (±0.3) wt%. Total not corrected for O ≡ F.

alytical data for ingersonite initially seemed to be consistent with these relations, they were normalized to 24 total A and B cations, the sum corresponding to the cell contents (see XRD data below) for the ideal pyrochlore composition. Analysis 3 in Table 1, which was obtained from the same crystal used for single-crystal studies, gave rise to the formula $(Ca_{9.02}Mn_{2.98})_{\Sigma=12}(Sb_{11.41}Mn_{0.28}Mg_{0.19}Fe_{0.11})_{\Sigma=11.99}O_{41.11}F_x$, where x is less than 4. F is variable (Table 1) and not included in our calculations.

The smaller Mg and Fe ions are assumed to occupy the smaller, octahedrally coordinated site, as there is a deficiency of Sb atoms. Because the amounts of Ca and Mn initially assigned to the A site exceeded the allowed sum, the excess Mn was also assigned to the B site, as Mn is smaller than Ca and is more likely to assume octahedral coordination.

Natural members of the pyrochlore family commonly have defects on the A, B, and anion sites. In addition, Sb may be in part trivalent, as proposed for stibiconite (Vitaliano and Mason, 1952) and confirmed by Mössbauer studies (Brisse et al., 1972); as such, it may occupy the A site. It is therefore not possible to normalize the formula to any specific cation or anion sum with complete confidence. The cell contents as calculated above (assuming no cation vacancies) are compatible with the pyrochlore formula, giving the ideal formula $(Ca_3Mn)Sb_4O_{14}$ for Z = 3. Alternative calculations based on other cation or anion sums, with or without vacancies, all give rise to detailed formulae that are only slightly different from that given above, and all are consistent with the same idealized formula.

X-RAY CRYSTALLOGRAPHY

Ingersonite was studied using Weissenberg and precession single-crystal X-ray methods. The diffraction photographs display an unusual pattern of systematic absences in that only every third reflection along c^* is observed for rows having $h,k = 2N$. Such reflections are very intense, implying a substructure. Together with one-third of the reflections in the parallel rows (having h or $k = 2N + 1$), these reflections define a pseudocubic, face-centered lattice with $a \approx 10.2$ Å, as only substructure reflections occurred in the X-ray diffraction pattern. Pyrochlore, and specifically the chemically related species romeite (see below), has a face-centered unit cell of equivalent dimensions. These relations, in combination with the chemical data, therefore imply that ingersonite has a structure that is derivative from that of romeite. Exceptions to the systematic extinction rule that are not compatible with any space group were not detected. Because such patterns often imply the presence of twinning, the diffraction patterns were examined for twinning, but none was detected.

The Laue symmetry is $\bar{3}2/m$, the lattice is primitive, and the presence of diagnostic reflections shows that there is no c glide. However, the general systematic extinction rule described above includes $00l$ reflections as a special case; this suggests that the apparently extinct $00l$ reflections may be weak but unobservable, as is true for the more general set of reflections. With this ambiguity taken into account, the list of possible space groups is $P3m$, $P32$, $P\bar{3}m$, $P3_12$, or $P3_22$.

The unit-cell parameters [$a = 7.287(3)$, $c = 17.679(9)$ Å, $V = 813.0(6)$ Å^3] were refined using powder data obtained with a 114.6-mm-diameter Gandolfi camera, powdered sample, NBS Si as an internal standard, and Cu$K\alpha$ X-radiation. The powder pattern of ingersonite (Table 2) was indexed by analogy with the pattern of romeite, but by taking the splitting of reflections due to the deviation from cubic symmetry into account. Several reflections occurring in the pattern of ingersonite, but not in that of romeite, are readily indexed on the calculated pattern of romeite. In addition, the single-crystal diffraction intensity relations implied that only the intense substructure reflections (i.e., those corresponding to the romeite unit cell) should be observable in the powder pattern. The reflections were indexed using the initial values of a and c as obtained from single-crystal diffraction photographs. A sufficient number of unambiguously indexed reflections were identified for least-squares refinement of the lattice parameters. However, even with the absence of superstructure reflections in the powder pattern, there is multiple indexing of many reflections. It is also interesting to note that because re-indexing of the face-centered pyrochlore lattice on hexagonal axes gives rise to a rhombohedral lattice, the presence of substructure reflections in the powder-diffraction pattern implies that ingersonite is pseudo–R-centered.

PHYSICAL PROPERTIES

Ingersonite occurs as massive aggregates of subhedral crystals, 2–3 mm in diameter, composed of 0.3–mm crystals intimately associated with filipstadite, a new Mn-Sb spinel-group mineral (Dunn et al., 1988). Ingersonite is brownish yellow, as is its streak. The luster is vitreous. Micro-indentation hardness was established using a Leitz Durimet micro-hardness tester, equipped with a Vickers indenter. VHN_{100} is 974–1097 (mean of 10 indentations is 1047). The indentations were slightly fractured at their corners and had concave outlines. Cleavage is perfect on

TABLE 2. X-ray powder diffraction data

Romeite				Ingersonite				Romeite				Ingersonite			
I/I_0*	d_{obs}	d_{calc}**	hkl	I/I_0*	d_{obs}	d_{calc}**	hkl	I/I_0*	d_{obs}	d_{calc}**	hkl	I/I_0	d_{obs}	d_{calc}**	hkl
60	5.92	5.94	111	20	5.89	5.94	101	20	1.340	1.338	355, 137	5	1.336	1.341	413
						5.89	003							1.340	325
				10†	5.12	5.14	102							1.338	407
				10	3.62	3.62	104							1.336	229
						3.57	111							1.333	21, 11
50	3.10	3.10	113	20	3.10	3.11	201							1.329	10, 13
						3.10	113	10	1.286	1.285	800	10†	1.283	1.284	408
						3.08	105	2	1.188	1.187	555, 157				
100	2.971	2.968	222	100	2.965	2.972	202	30	1.180	1.179	266	20	1.181	1.182	422
						2.947	006							1.177	40, 10
30	2.572	2.570	400	40†	2.565	2.568	204					2	1.174	1.172	20, 14
5	2.361	2.358	331					30	1.150	1.149	048	20†	1.152	1.151	424
				1	2.093	2.104	300					20†	1.146	1.146	22, 12
						2.099	124	5	1.130	1.128	119, 357				
						2.086	108	5	1.078	1.078	139				
20	1.979	1.978	115, 333	2	1.965	1.981	303	30	1.049	1.049	448	20	1.051	1.052	600
						1.977	125							1.050	428
						1.972	027					5	1.043	1.043	20, 16
						1.964	009	5	1.034						
70	1.819	1.817	440	50†	1.820	1.822	220	2	0.995						
				50†	1.810	1.810	208	20	0.9898			30	0.9894		
20	1.738	1.738	135	2	1.742	1.742	311	1	0.9586						
						1.741	223	2	0.9271						
						1.734	217	5	0.9092			5	0.9110		
				1	1.714	1.729	119	5	0.8986			2	0.9048		
5	1.568	1.568	335					2	0.8723			10	0.8706		
80	1.550	1.550	226	60	1.549	1.553	402	30	0.8693			2	0.8669		
						1.550	226					10	0.8641		
				40	1.543	1.542	20, 10	20	0.8571			5	0.8586		
10	1.484	1.484	444	10†	1.486	1.486	404					10	0.8560		
				2†	1.474	1.473	00, 12	2	0.8481						
10	1.440	1.438	117, 155					5	0.8260						
				1	1.429	1.443	321	10	0.8129			10	0.8135		
						1.441	405					10	0.8102		
						1.439	317	5	0.7862			5	0.7856		
						1.436	405	20	0.7840			10	0.7842		
						1.432	20, 11					2	0.7780		
												5	0.7773		
								10	0.7748			10	0.7750		

Note: Reflections coupled by parentheses are doublets, equivalent to a single reflection in the pattern of cubic romeite.
* Intensities visually estimated.
** *d* values calculated based on $a = 10.2802$ Å for romeite; $a = 7.287$, $c = 17.679$ Å for ingersonite.
† Reflections used in least-squares refinement.

{0001} and easily produced. Other cleavage observations are noted. Cleavage, however, is not useful as a discriminant for distinguishing ingersonite from romeite, because some "romeites" have distinct {111} cleavage or parting. The density was not measured because of the impure nature of the aggregates and because the density ($D_{calc} = 5.42$ g/cm^3) exceeds the limits of heavy-liquid techniques.

Qualitative optical properties

In isolation, in plane-polarized light (with a color temperature of about 3100 K), ingersonite is light gray, sometimes with a slight yellowish cast impaired by the yellow and white internal reflections that are characteristic of the mineral. When immersed in oil ($N_D = 1.515$), these internal reflections mask the surface color of all but the thickest grains, most of which have hexagonal outlines (Fig. 1A), are probably basal sections, and are dark gray. Even in these grains, internal reflections are not entirely absent, but are much less intense and are varicolored. Neither bireflectance nor reflectance pleochroism is apparent, and there is no evidence for twinning.

In plane-section, ingersonite is euhedral to subhedral; individual crystals are predominantly rectangular, generally elongate, giving the appearance of a prismatic, acicular, or bladed habit. The largest crystals are 0.4 mm long; some occur in isolation in the calcite matrix (which fluoresces strongly), but most cluster together in aggregates up to 3 mm across (Fig. 1F) and are intergrown with filipstadite and rounded grains of possible clinohumite (Fig. 1C). In this association, ingersonite appears a slightly darker gray than filipstadite and much darker than jacobsite.

Ingersonite has a perfectly developed basal cleavage and an imperfect rhombohedral cleavage; uneven fractures are common; a few are straight, but most are arcuate. Replacement of ingersonite by calcite is pervasive: the two minerals interdigitate raggedly (Fig. 1D). Replacement along the basal cleavage is common, in extreme cases

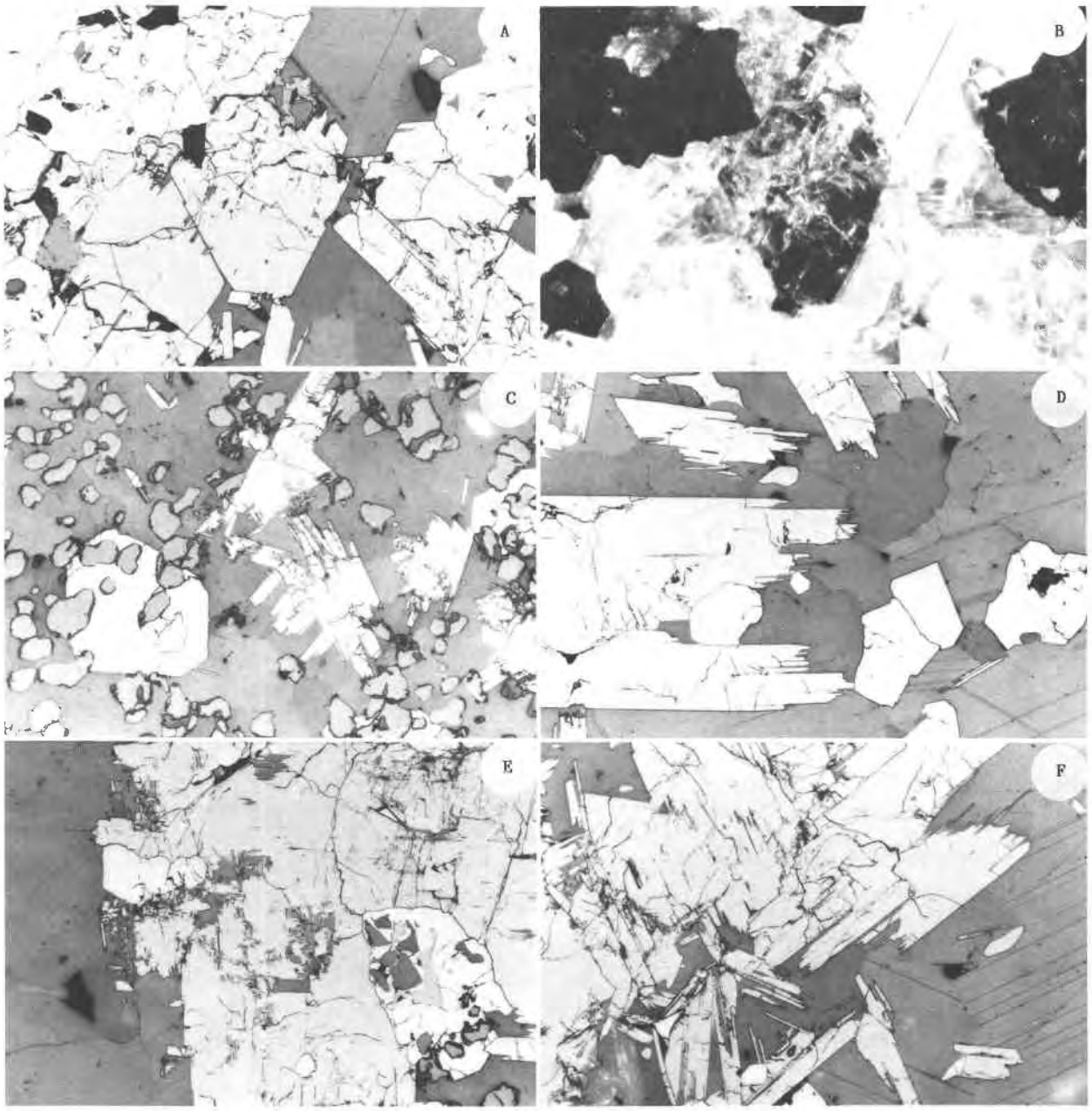

Fig. 1. Photomicrographs of ingersonite. The scale is constant (horizontal field is 500 μm) for all photomicrographs. (**A**) Plane-polarized light. Ingersonite crystal with an imperfect hexagonal outline, which is probably a basal section (midgray), in calcite (dark gray), intergrown with other ingersonite crystals and an unknown Mn-Sb-Fe oxide (slightly lighter gray) and jacobsite (white). (**B**) The same area as shown in (A), but between crossed polarizers, illustrating the difference in the internal reflections of the supposed basal section and other, randomly oriented sections. (**C**) Plane-polarized light. Ingersonite crystals (light gray) in calcite (dark gray) with abundant, rounded, grains of possible clinohumite (midgray) and a subhedral crystal of jacobsite (white). (**D**) Plane-polarized light. Laths of ingersonite, interdigitating with calcite (dark gray). Some angular grains of filipstadite (one with a "core" of jacobsite) are also present in the calcite. (**E**) Plane-polarized light. Ingersonite showing partial replacement along its two cleavages by calcite. A complex intergrowth of jacobsite (white), possible clinohumite (midgray), calcite (dark gray), and filipstadite (lighter gray) is included in the ingersonite intergrowth. (**F**) A cluster of ingersonite crystals (light gray) in calcite (dark gray).

leading to relict textures where only a few laths of ingersonite remain; in a few crystals, "boxlike" textures result (Fig. 1E) from replacement along both the basal and rhombohedral cleavages.

Between crossed polarizers, the yellow and white internal reflections of ingersonite are intense for all but the hexagonal sections (Fig. 1A, 1B). These appear dark gray but do not extinguish because of the presence of feeble,

"rainbowlike," internal reflections. In a few of the thickest prismatic sections, the color of the internal reflections is dark brown. Anisotropic rotation tints, if present, are masked by the internal reflections.

In transmitted light, ingersonite is medium to light yellow in color; pleochroism is not discernible or absent. The mineral is uniaxial, negative.

Reflectance, color values, and optical constants

Several areas of a polished sample (BM 1986, 410: E.1177) were analyzed by microprobe prior to reflectance measurement; the analyses (nos. 1 and 2, Table 4) proved ingersonite to have a fairly constant chemical composition, and seveal areas were selected as suitable for reflectance measurement. The sample was cleaned and buffed by hand with a slurry of MgO in distilled water.

Reflectance measurements were made with the equipment of, and using the procedures described by, Criddle et al. (1983). A Zeiss SiC standard (no. 472) was used; the microscope was adjusted to provide effective numerical apertures of 0.15 for the ×16 air and oil objectives, and Zeiss oil (N_D = 1.515) was used for the immersion measurements. The reflectance values are given in Table 3 (nos. 1 and 2 in Table 3 correspond to nos. 1 and 2 in Table 1).

It is difficult to obtain reliable and consistent reflectance measurements from ingersonite: internal reflections prevent the identification of extinction positions and add a spurious component to the surface reflectance. This component may be considered as an increment from simple or multiple reflections from the lower surface of the crystal and from any fractures it contains; as such, it will vary with the thickness of the crystal. Three crystals were measured in this investigation. Two lacked any apparent internal reflections (that is not to say that they were entirely absent); the third possessed intense internal reflections. The first two appeared light gray in plane-polarized light; the third was more highly reflecting and, when immersed in oil, was distinctly yellowish in comparison. All three crystals were aligned with respect to their basal cleavage, and the orientation of the maximum and minimum reflectances used for measurement was determined photometrically.

The visual phenomena described above are confirmed by the measured reflectance spectra (Fig. 2). The spectra of the grains lacking internal reflections are remarkably similar and are weakly dispersed with a gentle reduction in reflectance from the blue to red end of the spectrum. In comparison, the spectra of the internally reflecting grain are even less dispersed in air and are slightly higher reflecting for most of the spectrum. The yellowness observed in oil is explained by the rapid increase in the reflectance from 400 to 500 nm and the gradual, if slight, increase to 700 nm.

Color values derived from these spectra (Table 4) are in complete agreement with the qualitative observations. The luminance [Y (%)] for the internally reflecting grain (grain 3) is 0.5% (5% relative) higher in air, and 0.6 to 0.9% (40 to 60% relative) higher in oil than the luminance of the other grains. There is little difference between the dominant wavelengths (hue), or excitation purities (saturation) of the three grains in air, but marked differences in oil: the λ_d value for grain 3 is in the yellow sector of the color diagram, the λ_d values for grains 1 and 2 are in the blue sector, and the P_e (%) value for grain 3 is substantially higher than for the other grains.

TABLE 3. Reflectance data for ingersonite

λ	1		2		1		2	
(nm)	R_1	R_2	R_1	R_2	$^{im}R_1$	$^{im}R_2$	$^{im}R_1$	$^{im}R_2$
400	11.16	11.40	10.98	11.03	1.74	1.76	1.67	1.68
410	11.05	11.25	10.86	10.90	1.70	1.74	1.64	1.66
420	10.94	11.13	10.75	10.80	1.66	1.71	1.61	1.64
430	10.85	11.03	10.65	10.70	1.63	1.68	1.59	1.62
440	10.74	10.88	10.56	10.61	1.61	1.66	1.56	1.60
450	10.62	10.76	10.48	10.53	1.58	1.63	1.54	1.59
460	10.52	10.66	10.40	10.45	1.56	1.61	1.52	1.58
470	10.43	10.56	10.34	10.39	1.54	1.59	1.51	1.58
480	10.34	10.48	10.28	10.34	1.52	1.57	1.50	1.58
490	10.26	10.40	10.23	10.29	1.51	1.55	1.50	1.58
500	10.18	10.32	10.18	10.23	1.49	1.54	1.49	1.58
510	10.12	10.25	10.12	10.18	1.48	1.53	1.48	1.57
520	10.05	10.19	10.07	10.13	1.47	1.52	1.48	1.57
530	10.00	10.13	10.02	10.08	1.47	1.51	1.48	1.56
540	9.96	10.09	9.98	10.05	1.46	1.50	1.47	1.55
550	9.93	10.06	9.95	10.02	1.45	1.49	1.47	1.55
560	9.91	10.04	9.92	10.00	1.45	1.49	1.46	1.55
570	9.89	10.02	9.91	9.99	1.44	1.49	1.46	1.54
580	9.89	10.01	9.90	9.98	1.44	1.49	1.46	1.55
590	9.89	10.01	9.90	9.98	1.44	1.49	1.46	1.55
600	9.89	10.02	9.90	9.98	1.44	1.49	1.46	1.55
610	9.89	10.02	9.91	9.98	1.44	1.49	1.47	1.55
620	9.90	10.03	9.92	9.99	1.44	1.49	1.47	1.55
630	9.90	10.03	9.92	9.99	1.45	1.50	1.48	1.55
640	9.90	10.03	9.93	10.00	1.45	1.50	1.48	1.56
650	9.91	10.03	9.93	10.00	1.45	1.50	1.48	1.56
660	9.91	10.03	9.93	10.00	1.45	1.50	1.49	1.56
670	9.91	10.03	9.92	9.99	1.46	1.50	1.49	1.56
680	9.91	10.03	9.91	9.98	1.46	1.50	1.49	1.55
690	9.91	10.03	9.90	9.97	1.46	1.50	1.49	1.55
700	9.91	10.03	9.89	9.96	1.45	1.50	1.49	1.55

It should be noted that the general symbols R_1 and R_2 are used in Table 1; R_o and R_e could not be determined from the reflectance measurements because of the very weak birefringence of ingersonite and because of the uncertainty about its extinction properties (the reflectance data for grain 3 are not included in Table 1 because they are clearly erroneous).

We have dwelt on the subject of internal reflections at some length because their effects in ingersonite perfectly illustrate the need for caution when using reflectance data to derive the optical constants of highly refracting transparent minerals.

Application of the two-media method for deriving optical constants produced results that are at variance with the observed transparency of the mineral. The Koenigsberger equations yielded absorption coefficients of 0.0 to 0.2 for grains 1 and 2 and 0.4 for grain 3. The erroneously high absorptions for grains 1 and 2 (i.e., 0.2) may be

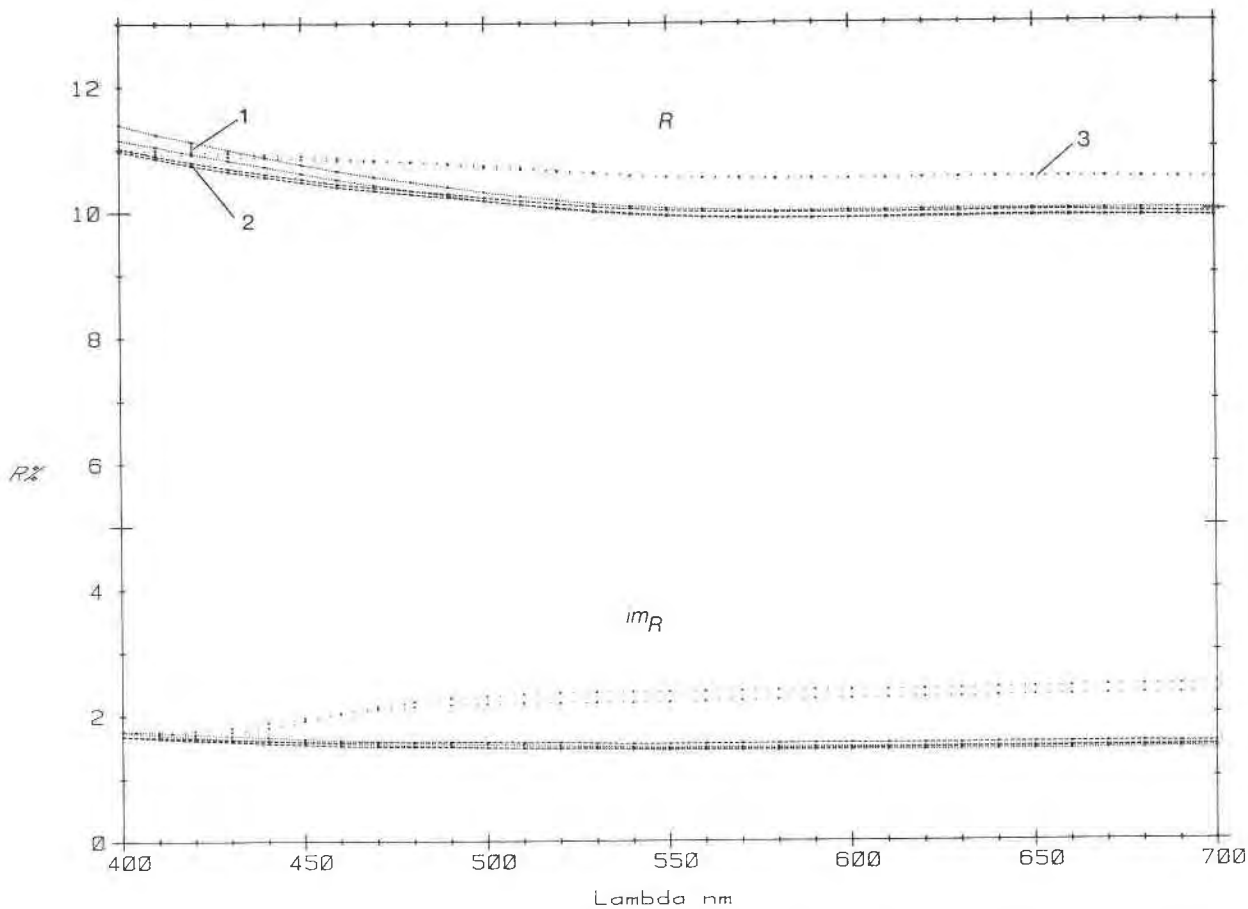

Fig. 2. Measured reflectance spectra for ingersonite. R refers to the spectra in air, and ^{im}R in oil (N_D = 1.515). The ornament used is the same for both R and ^{im}R. Nos. 1, 2, and 3 are for the grains referred to in the text and tabulated data.

attributed, in part, to measurement error and, in part, to the contribution made to the surface reflectance by internal reflections. Errors resulting from the latter would be greater if, in relative terms, the contribution to the oil reflectance were higher than to the air reflectance—as is demonstrably the case for grain 3. The refractive indices calculated for grains 1 and 2 using the Koenigsberger equations were compared with those obtained with the Fresnel equation (assuming $k = 0$), as recommended by Embrey and Criddle (1978). In Table 5, the mean of the refractive indices so derived from the R and ^{im}R values are compared, for a few wavelengths, with those derived using the Koenigsberger equation. The discrepancy between the two sets of derived values is generally smaller for grain 1 than

TABLE 4. Color values of ingersonite

	1		2		3		1	
	R_1	R_2	R_1	R_2	R_1	R_2	$^{im}R_1$	$^{im}R_2$
				Relative to illuminant C at 6774 K				
x	0.3047	0.3046	0.3059	0.3060	0.3074	0.3077	0.3030	0.3030
y	0.3085	0.3084	0.3107	0.3105	0.3130	0.3137	0.3061	0.3060
Y (%)	10.0	10.1	10.0	10.1	10.6	10.6	1.5	1.5
λ_d	469	469	471	471	473	476	469	468
P_e (%)	3.0	3.0	2.3	2.2	1.4	1.2	3.9	3.9
				Relative to illuminant A at 2856 K				
x	0.4432	0.4431	0.4440	0.4441	0.4451	0.4452	0.4420	0.4420
y	0.4045	0.4045	0.4055	0.4054	0.4064	0.4068	0.4034	0.4033
Y (%)	9.9	10.1	10.0	10.0	10.6	10.6	1.5	1.5
λ_d	482	483	484	484	487	489	481	481
P_e (%)	1.2	1.2	0.9	1.0	0.6	0.6	1.6	1.6

Note: The values for grains 1 and 2 were derived from the data in Table 3; those for grain 3 are for the internally reflecting grain (the reflectance data

for grain 2, suggesting that, if ingersonite is truly transparent (or weakly absorbing), the data for grain 1 are the more reliable.

The Gladstone-Dale relationship

Application of the Gladstone-Dale relationship produces some interesting and encouraging results. The revised Gladstone-Dale constants (Mandarino, 1981) were used. The value K_C derived from the ideal formula is 0.1674; those derived from the analyses of grains 1 and 2 are 0.1666 and 0.1665, respectively. The K_P value for $n = 1.91$ (assuming $k = 0$) for the ideal formula is 0.1676, and the K_P values for grains 1 and 2, using the microprobe data in Table 2, are 0.1667 and 0.1670. The corresponding values for $n = 1.93$ (using the Koenigsberger equations) are 0.1713, 0.1703, and 0.1706.

The compatibility index (Mandarino, (1979) for $n = 1.93$ is -0.023 for the ideal composition (-0.022 for grain 1 and -0.025 for grain 2), excellent in the subjective terminology of Mandarino (1979); for $n = 1.91$, the indices are -0.001, -0.001, and -0.003, respectively (all superior).

Discussion

The formula of ingersonite can be written $(Ca,Mn)_4Sb_4O_{14}$, to a first approximation, as compatible with the diffraction relations that imply that it has a structure derivative from that of pyrochlore (Zedletz, 1932). However, Byström (1944a) showed that synthetic $Ca_2Sb_2O_7$ has the weberite crystal structure, as determined by Byström (1944b). This was confirmed by Butler et al. (1950), among others. On the other hand, Brisse et al. (1972) and Knop et al. (1980) synthesized $Ca_2Sb_2O_7$ with both pyrochlore and weberite structures. Brisse et al. (1972) concluded that the weberite structure is favored by high temperature. They also synthesized $Mn_2Sb_2O_7$ with the pyrochlore structure.

Knop et al. (1980) have reviewed the factors controlling formation of a given antimonate with the pyrochlore versus the weberite structures, noting that ionic radius and electronegativity of the A cation are the principal determining factors. Plots of these variables versus structure type define weberite and pyrochlore fields, with $Ca_2Sb_2O_7$ being in the transition zone, as consistent with its synthesis in both structure types. On the other hand, $Mn_2Sb_2O_7$ plots well within the pyrochlore field. The pyrochlore-like structure of ingersonite $Ca_3MnSb_4O_{14}$ is therefore consistent with these relations.

Zedletz (1932) concluded that F is essential to the pyrochlore structure. Similar conclusions were reached by Butler et al. (1950) and Aia et al. (1963), who showed that substitution of even small amounts of F in $Ca_2Sb_2O_7$ gives rise to the pyrochlore structure. Variable but significant amounts of F occur in ingersonite, as described above, as consistent with a pyrochlore-derivative structure.

Although pyrochlore-type structures are usually cubic, derivative structures having space groups that are subgroups of the space group of pyrochlore, $Fd3m$, are not uncommon (e.g., Subramanian et al., 1983). Knop et al. (1980) have noted that such relations may be caused by (1) trigonal distortions due to electron lone-pair effects where the A site is occupied by Pb, (2) nonstoichiometry such that vacancies may occur on the A, B, or anion sites, and (3) ordering of cations on A sites. The mineral parabariomicrolite (Ercit et al., 1986) exemplifies the ordered-vacancy mechanism; vacancies on the A sites give rise to the space group $R\bar{3}m$ with lattice parameters $a = 7.4290$, $c = 18.505$ Å. Curiously, this cell has the same approximate dimensions as that for ingersonite, although it is rhombohedral whereas the unit cell of ingersonite is primitive. Cation ordering on the A site is exemplified by solid solutions of the type $(Cd,Sr)_2Sb_2O_7$, for which ordering occurs for equal amounts of Cd and Sr (Desgardin et al., 1976).

Of these known causes of derivative symmetry relations in pyrochlore-structure compounds, the lone-pair and vacancy mechanisms have no apparent application to ingersonite. On the other hand, in ingersonite the ratio of A-site cations Ca:Mn = 3:1 is consistent with ordering of those cations. The atom ratio is compatible with space-group equipoint ranks among the possible space groups. This relation is problematical at best, however, and its verification must await a structure analysis.

Romeite is a member of the pyrochlore group that has

TABLE 4—*Continued*

2		3	
$^{im}R_1$	$^{im}R_2$	$^{im}R_1$	$^{im}R_2$
0.3081	0.3065	0.3203	0.3246
0.3134	0.3105	0.3309	0.3400
1.5	1.6	2.2	2.4
464	469	573	571
2.1	1.1	6.7	10.3
0.4458	0.4449	0.4548	0.4570
0.4065	0.4052	0.4128	0.4167
1.5	1.6	2.2	2.4
485	479	583	581
0.8	0.5	8.7	13.0

for which are not tabulated as they are erroneous).

TABLE 5. Indices of refraction for ingersonite

	1		2		1		2	
λ (nm)	n_1	n_2	n_1	n_2	n_1	n_2	n_1	n_2
400	2.01	2.01	1.99	1.99	2.01	2.01	1.99	2.00
450	1.97	1.98	1.95	1.95	1.97	1.98	1.96	1.97
470	1.95	1.96	1.94	1.94	1.96	1.97	1.95	1.96
500	1.93	1.94	1.93	1.92	1.94	1.95	1.94	1.95
550	1.91	1.92	1.91	1.90	1.93	1.94	1.93	1.94
590	1.91	1.91	1.90	1.90	1.92	1.93	1.93	1.94
600	1.91	1.92	1.90	1.90	1.92	1.93	1.93	1.93
650	1.91	1.92	1.91	1.90	1.92	1.93	1.93	1.93
700	1.91	1.92	1.91	1.90	1.92	1.93	1.93	1.93

Note: The first four columns are the n values derived from the reflectances in two media using the Koenigsberger equations. The last four columns are the mean values from the air and oil reflectances calculated using the Fresnel equation, i.e., assuming zero absorption.

a formula, $(Ca,NaH)Sb_2O_6(O,OH,F)$, closely related to that of ingersonite (Vitaliano and Mason, 1952). As part of a more general investigation of pyrochlore-family relations, we have verified by single-crystal diffraction relations that it has space group $Fd3m$ (unpub. data). Although there are vacancies on the A site resulting in a lack of complete analogy to ingersonite, these data further imply that the derivative structure of ingersonite is unique to its composition.

Acknowledgments

This manuscript was greatly improved by the reviews of T. Scott Ercit and Frank C. Hawthorne.

References cited

Aia, M.A., Mooney, R.W., and Hoffman, C.W.W. (1963) An X-ray study of pyrochlore fluorantimonates of calcium, cadmium and manganese. Electrochemical Society Journal, 110, 1048–1054.

Brisse, F., Stewart, D.J., Seidl, V., and Knop, O. (1972) Pyrochlores. VIII. Studies of some 2-5 pyrochlores and related compounds and minerals. Canadian Journal of Chemistry, 50, 3648–3666.

Butler, K.H., Bergin, M.J., and Hannaford, V.M.B. (1950) Calcium antimonates. Electrochemical Society Journal, 97, 117–122.

Byström, A. (1944a) X-ray analysis of $Ca_2Sb_2O_7$ and compounds of similar composition. Arkiv för Kemi, Mineralogi och Geologi, 18A, 1–8.

——— (1944b) The structure of weberite, Na_2MgAlF_7. Arkiv för Kemi, Mineralogi och Geologi, 18, 1–7.

Criddle, A.J., Stanley, C.J., Chisholm, J.E., and Fejer, E.E. (1983) Henryite, a new copper-silver telluride from Bisbee, Arizona. Bulletin de Minéralogie, 106, 511–517.

Desgardin, C., Robert, C., and Raveau, B. (1976) Influence de la nature des ions et sur l'évolution structurale des weberites $A_2B_2O_7$: Les weberites $Cd_2 - {}_xSr_xSb_2O_7$. Canadian Journal of Chemistry, 54, 1665–1671.

Dunn, P.J., Peacor, D.R., Criddle, A.J., and Stanley, C.J. (1988) Filipstadite, a new $Mn\text{-}Fe^{3+}\text{-}Sb$ derivative of spinel, from Långban, Sweden. American Mineralogist, 73, 413–419.

Embrey, P.G., and Criddle, A.J. (1978) Error problems in the two-media method of deriving the optical constants n and k from measured reflectances. American Mineralogist, 63, 853–862.

Ercit, T.S., Hawthorne, F.C., and Černý, P. (1986) Parabariomicrolite, a new species and its structural relationship to the pyrochlore group. Canadian Mineralogist, 24, 655–663.

Knop, O., Demazeau, G., and Hagenmuller, P. (1980) Pyrochlores. XI. High-pressure studies of the antimonates $A_2Sb_2O_7$ (A = Ca,Sr,Cd) and preparation of the weberite $Sr_2Bi_2O_7$. Canadian Journal of Chemistry, 58, 2221–2224.

Mandarino, J.A. (1979) The Gladstone-Dale relationship. Part III: Some general applications. Canadian Mineralogist, 17, 71–76.

——— (1981) The Gladstone-Dale relationship. Part IV. The compatibility concept and its application. Canadian Mineralogist, 19, 441–450.

Subramanian, M.A., Aravamudan, G., and Rao, G.V.S. (1983) Oxide pyrochlores—A review. Progress in Solid State Chemistry, 15, 55–143.

Vitaliano, C.J., and Mason, B. (1952) Stibiconite and cervantite. American Mineralogist, 37, 982–999.

Zedletz, O. (1932) The crystal structure of romeite and schneebergite. Zeitschrift für Kristallographie, 81, 253.

Manuscript received February 27, 1987
Manuscript accepted November 20, 1987